Journal of Applied Mechanics and Technical Physics, Vol. 42, No. 1, pp. 35–41, 2001

SUDDEN BLOCKING OF A SUBCRITICAL OPEN-CHANNEL FLOW

V. I. Bukreev and V. A. Kostomakha

UDC 532.59

This paper reports results of experiments in which a steady nonuniform flow in a rectangular channel with an even horizontal bottom was blocked by a rapidly falling shield. Data on the height of the splash-up of water on the shield and the shape, propagation speed, height, and internal structure of the upstream propagating wave of the bore type are obtained for various liquid flow rates at the channel entrance. It is established that the bore produces a strong stratification in the liquid particle velocity, and under particular conditions, the speed of propagation and height of the bore, and the height of the water splash-up on the wall are constant and are determined only by the critical depth for unperturbed flow, i.e., by the specified flow rate.

Entering a river, a tidal wave or a tsunami wave can be transformed into a moving hydraulic jump, which is termed a "bore" [1]. Only descriptive information on this complex process has been obtained previously [2]. Much more attention has been given to waves of the bore type in the dam-break problem [1]. A characteristic feature of the transformation of a tidal wave is that this wave propagates over a counterflow. Because of nonlinearity, nonstationarity, and possibility of breaking, a theoretical analysis of waves of the bore type involves great difficulties. Therefore, information on these waves can be obtained mainly in physical and numerical experiments.

The present paper reports results of laboratory studies of the formation and propagation of a bore over a counterflow in a simple formulation of the problem. The experimental setup is shown schematically in Fig. 1. A steady flow of an incompressible liquid (water) with volume flow rate Q was produced in a rectangular channel of width B with an even horizontal bottom. At the time $t = 0$, the channel flow was completely blocked by a rapidly falling shield with cross section $x = 0$. The fixed rectangular coordinate system used is shown in Fig. 1.

In hydraulics, important characteristics of the unperturbed flow considered are the critical depth h_* and the corresponding critical speed V_*, which are given by the formulas [3, 4]

$$h_* = \sqrt[3]{q^2/g}, \qquad V_* = \sqrt{gh_*}, \qquad q = Q/B,$$

where q is the specific flow rate and g is the acceleration of gravity. A flow is called subcritical if its local depth $h(x)$ exceeds h_*. In the present paper, we consider the case where the shield blocks a subcritical flow. The unperturbed free surface was a decrement curve, the local depth $h(x)$ decreased monotonically, and the local velocity $V = Q/(Bh)$ increased monotonically downstream.

When the shield fell, a bore type wave propagated upstream. An important difference between a bore and a classical hydraulic jump is that the former is substantially unstationary. In the present experiments, the bore propagated over a shear counterflow with increasing depth. There are five main forms of a classical hydraulic jump produced by flow from under a shield [4]. All these forms were observed in the present experiments. Three of them are characterized by the presence of undulations — gradually damped oscillations of the free surface. The undular bore was smooth or had a breaking first crest or several breaking crests.

Lavrent'ev Institute of Hydrodynamics, Siberian Division, Russian Academy of Sciences, Novosibirsk 630090. Translated from Prikladnaya Mekhanika i Tekhnicheskaya Fizika, Vol. 42, No. 1, pp. 40–47, January–February, 2001. Original article submitted March 14, 2000; revision submitted July 6, 2000.

0021-8944/01/4201-0035 $25.00

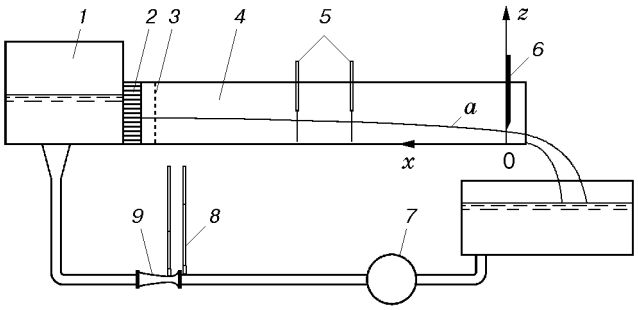

Fig. 1. Experimental setup: 1) damping reservoir; 2) honeycomb; 3) perforated plate; 4) working section of the channel; 5) wavemeters; 6) shield; 7) pump; 8) water pressure gauge; 9) Venturi meter; a is a decrement curve.

Generally, besides B, Q and g, among the parameters of the problem considered are the density ρ and kinematic viscosity ν of the liquid, surface tension, and the density, viscosity, and compressibility of air. Below, we consider only flow kinematic characteristics on which densities of water and air have only indirect influence via the mechanism of energy dissipation and only in the case where waves break and air is entrained in the water. Surface tension and the viscosity and compressibility of air were of secondary significance in the experiments. The main parameters were B, Q, g, and ν. They can be united in two independent dimensionless complexes, for example,

$$\Pi_1 = \frac{Q}{B^2\sqrt{gB}}, \qquad \Pi_2 = Q\sqrt[3]{\frac{g}{\nu^5}}.$$

In the present experiments, Π_1 and Π_2 were related to one another because $B = 6$ cm and $\nu = 0.0115$ cm^2/sec did not change. Therefore, below we give only values of Π_1. If necessary, from the values of Π_1 and B, one can calculate the flow rate and then Π_2. The effects of surface tension and air can be taken into account by using reference data for them at a temperature of 15°C. In the formulation of the problem, an important point is the choice of the cross section of the channel in which the shield falls. In the experiments described here, the shield was at a distance of 11 cm from the channel outlet section, where the water was freely issuing into the atmosphere.

The channel with a working section 4.8 m long had transparent Plexiglas walls. Unperturbed flow was produced by a bladed pump with a direct current electric motor. This made it possible to vary the flow rate over a wide range by changing the speed of the electric motor without using a value. The system incorporated a Venturi meter with a water pressure gauge. To flatten the flow at the entrance to the working section of the channel, we used a damping reservoir, a honeycomb, and a perforated plate. The shield was dropped manually for a typical time of about 0.1 sec. After the shield fell, the pump continued to work. Measurements were terminated when the reflected wave reached the shield.

In the experiments, we measured decrement curves $h(x, \Pi_1, \Pi_2)$, the height of the water splash-up on the fallen shield $H(y, \Pi_1, \Pi_2)$, and the wave profile $\eta(x, t, \Pi_1, \Pi_2) = z^* - h$, where z^* is the vertical coordinate of the perturbed free surface in the longitudinal plane of symmetry of the channel. The internal structure of the flow was also studied. The term "internal structure" is used here for an ensemble of trajectories of fine suspended particles (aluminum powder).

The decrement curves were measured by a measuring needle. The wave profile was determined by means of motionless wavemeters, which recorded the dependence of $\eta(t)$ for fixed values of other arguments, in particular, x. Two wavemeters spaced $\Delta x = 30$ cm apart measured the times Δt_i and rates of longitudinal displacements $c_i = \Delta x/\Delta t_i$ for a number of points chosen on the wave profile. Since the waves were non-stationary, different points of their profiles moved with different speeds. Under the conditions of the present experiments, the rates of displacement of points of the leading front differed by not more than 2%.

For measurements of H, a tooth-powder was applied on the shield surface by means of a porolon sponge. Upon reflection of the flow, the powder was flushed away, and a distinct boundary of the maximum

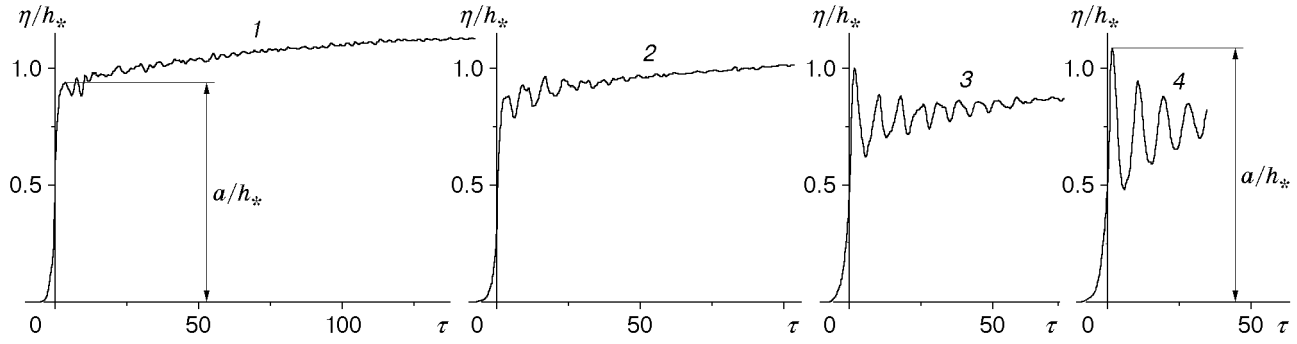

Fig. 2. Development of a bore for $\Pi_1 = 0.235$: curves 1–4 refer to $x/l = 0.55 \cdot 10^4$, $1.17 \cdot 10^4$, $1.80 \cdot 10^4$, and $2.42 \cdot 10^4$, respectively.

water splash-up remained on the shield surface. The trajectories of the aluminum powder particles were recorded by photography in a dark room. Only the chosen part of the flow in the neighborhood of the longitudinal symmetry plane of the channel was illuminated by a light "knife" about 1 cm thick. The exposure in photography was large (up to 1 sec).

Below, a denotes the height of the wave and c denotes the speed of wave propagation. In the presence of undulations, a was taken to be the height of the first wave crest, and in the absence of undulations, it was the difference of levels behind and ahead of the leading wave front. The speed of propagation means the value of c_i that corresponds to the point at the middle height of the leading wave front.

An analysis of several possible versions of conversion to dimensionless quantities shows that for the goals of the present work, various characteristic length scales are optimal: the critical depth h_* for h, η, H, and a, the channel width B for the transverse coordinate y, and the complex $l = C^{1/3}\nu^{2/3}g^{-1/2}$ for the longitudinal coordinate x (C [$\mathrm{m}^{1/2}$/sec] is the Chezi empirical coefficient, which takes into account the roughness of the channel walls [3, 4]). In a channel with zero slope of the bottom in experiments, the value of C is determined with a large error. Since the coefficient C is used below only for normalization, its value is calculated from the Manning formula [3, 4]. The coefficient C depends on Q and x. This dependence is weak, however. In the present experiments, the scale l was varied in the range 0.0126–0.0131 cm. Therefore in the normalization of x, we used the constant mean value of $l = 0.0128$ cm. The time was normalized by $\sqrt{h_*/g}$, and the speeds were normalized by $V_* = \sqrt{gh_*}$ and $\sqrt{gh}$.

Figure 2 shows typical wave profiles as functions of time recorded by the wavemeters in the same experiment at different distances from the shield. The quantity $\tau = (t - t_{0j})/\sqrt{h_*/g}$ is plotted on the abscissa (t_{0j} is the moment when the middle point of the leading front passes through the wavemeter).

Upon reflection from the shield, a turbulent bore with a breaking leading front and a roller in the head formed. Then undulations occurred, but the roller was maintained. With distance from the shield, the undulations strengthened and the breaking of the leading front became less intense. At large distances, the breaking ceased and a smooth undular bore formed. As in the cases of a classical wavy hydraulic jump [4] and a solitary wave [5], on the smooth, generally flat bore there were oblique waves, whose amplitudes was limited by surface tension. In the example considered, the leading front of the bore broke on the interval $0 < x/l < 1.8 \cdot 10^4$. On the interval $1.8 \cdot 10^4 < x/l < 2.4 \cdot 10^4$, the bore was smooth. Then, its leading front began to break again.

At the scale of Fig. 2, the difference between smooth and breaking waves is insignificant. Visually, the transition from smooth waves to breaking waves and the reverse transition was traced more precisely. Visual observations showed that in the initial stage of the direct transition and at the closing stage of the reverse transition, a typical bend — an angular point with the apex directed to the inside of the wave — appeared on the profile of the leading front of the undular bore (and not on the crest but closer to its trough). It is interesting to compare this result with the well-known data for solitary and undular waves on an initially quiescent liquid of constant depth.

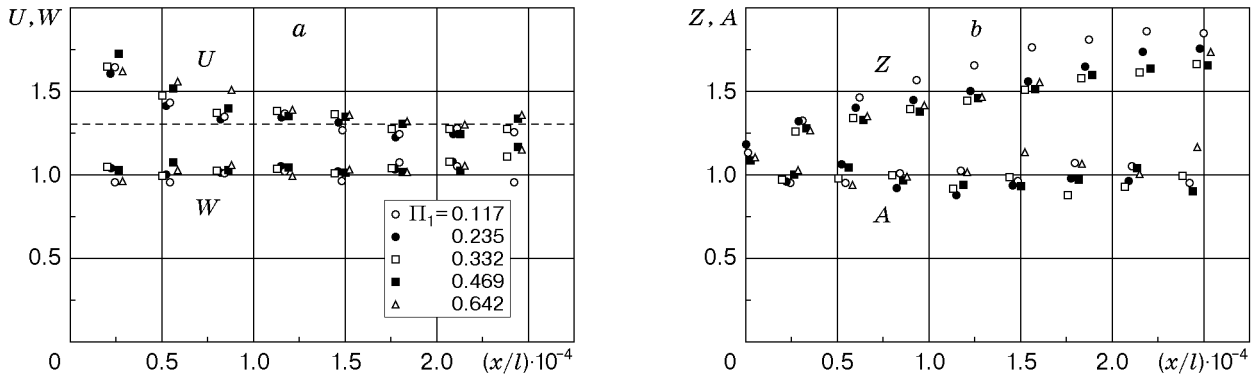

Fig. 3. Dependence of the characteristics of the main flow and the bore on x/l for $U = (c + V)/\sqrt{gh}$, $W = c/V_*$, $Z = h/h_*$, and $A = a/h_*$.

Theoretical calculations of a solitary wave of limiting amplitude have been performed in many papers (see, for example [6, 7]). In theory, the limiting state means a state in which the local velocity of the liquid particles coincides with the speed of wave propagation even at one point of the flow field. In the model of an ideal liquid, these speeds coincide at the crest, and it is precisely in this place that an angular point appears as an indication of the instability of the theoretical wave. In real waves, the picture is complicated by the influence of viscosity, surface tension, and the fact that on a plane solitary wave there are always oblique waves. Nevertheless, breaking of a real solitary wave begins from the crest. The experiments of [8] showed that this is also true for undular waves on a quiescent liquid. Therefore, the displacement of the angular point to the trough of the leading front observed in the present experiments is due to the influence of the counterflow.

The experiments performed provided some information on the conditions under which transition from smooth to breaking waves begins and the reverse transition ends in the presence of a counterflow. Investigation of this problem for waves propagating over a quiescent liquid with constant final depth h_0 showed (see [8]) that in this case, along with the well-known characteristic speed $c_1 = \sqrt{gh_0}$, there is the higher characteristic speed $c_2 = 1.294c_1$, in whose neighborhood direct and reverse transitions from breaking to smooth waves on shallow water occur in practice. For speeds close to c_1, the waves retain smoothness. In the range $c_1 < c < c_2$, on a smooth main wave there are oblique waves. The value of the coefficient of 1.294 was obtained by theoretical calculations for solitary waves [6], and its validity for waves of the type of a smooth undular bore was justified only by experiments.

One should expect that local (dependent on x) critical speeds with a similar physical meaning also exist for the problem considered, along with the critical speed V_* calculated from the specified flow rate. In determining these speeds, one should take into account the unperturbed flow velocity. As a first approximation, for waves on counterflow, the local critical speeds can be $c_*(x, \Pi_1, \Pi_2) = \sqrt{gh} - V$ and $c_{**}(x, \Pi_1, \Pi_2) = 1.3\sqrt{gh} - V$, and, in this case, both h, and V depend on x. To obtain more precise values for them, it is necessary to take into account the nonstationarity of the wave and the inhomogeneity of the counterflow along the three spatial coordinates.

Figure 3 gives experimental values of c as functions of $U(x/l)$ and $W(x/l)$. The first function is obtained with normalization of c by $\sqrt{gh}$, and the second is obtained with normalization by V_*. The second critical speed has a value of $U = 1.294$ (dashed curve), and the first critical speed has a value of $U = 1$. Visual observations showed that the experimental points U located above the dashed curve correspond to breaking waves, and the experimental points located below it correspond to smooth waves. Thus, within a root-mean-square measurement error of 2%, the experiments confirmed the assumption that for waves on counterflow, direct transition from smooth to breaking waves occurs in the neighborhood of the second local critical speed $c = c_{**}$. As in the case of propagation of undular waves on a quiescent liquid, the reverse transition ended at a value of c somewhat smaller than c_{**} but much larger than c_*.

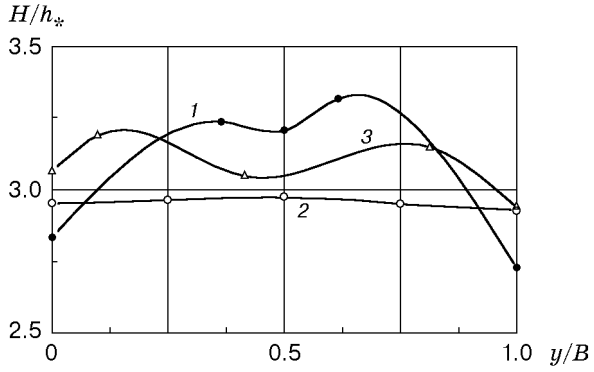

Fig. 4

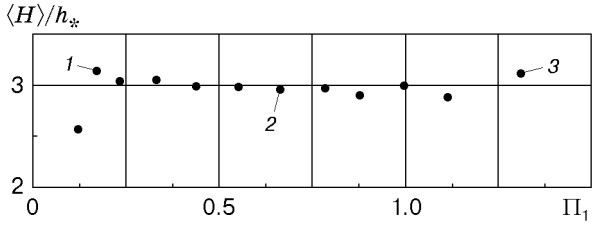

Fig. 5

Fig. 4. Typical profiles of the splash-up height for $\Pi_1 = 0.174$ (1), 0.665 (2), and 1.31 (3).

Fig. 5. Dependence of the mean height of splash-up on Π_1 (the chosen point numbers correspond to the profile numbers in Fig. 4).

Normalization by V_* yields the following important result: there is a range of Π_1 and x in which $c/V_* = \text{const}$, and, more interestingly, the value of the constant is close to unity. This implies that to determine the speed of propagation of the bore, it suffices to know only the flow rate. In theoretical calculations, this result can be used for testing models or as a postulate for closure of a system of equations. A more complete determination of the range of applicability of this postulate requires further examination. The experimental data given in Fig. 3a show that for small and large x there are some deviations from the regularity discussed here. For small x, the deviation is caused by the splash-up of water on the wall, and for large x, they are caused by the influence of undulations. One might expect that in the presence of strong undulations, the ratio c/V_* does not exceed 1.3.

The functions $Z(x/l)$ in Fig. 3b correspond to the decrement curves for the unperturbed flow. It should be noted that with the chosen direction of the x axis opposite to the main flow (see Fig. 1), these functions are a mirror reflection of the real decrement curves. It is obvious that normalization of h by h_* and normalization of x by l does not lead to the universality of the functions discussed. Determination of optimal normalization requires additional experimental information.

The indicated normalization is close to the optimum for the bore height, as follows from the dependence represented by the points A in Fig. 3b. As the propagation speed, the nondimensional height of the bore is constant in a certain range of Π_1 and x, and the value of the constant is close to unity. For the bore height, the spread of experimental points is somewhat larger than that for the propagation speed. For small x, there are deviations from the observed regularity due to the splash-up of water on the wall.

Figure 4 shows the dependence of the splash-up height on the longitudinal coordinate y for various values of the parameter Π_1. It is expedient to consider these data together with the dependence of the mean height of splash-up $\langle H\rangle$ on Π_1 given in Fig. 5. The experimental points 1–3 in Fig. 5 correspond to the curves with the same numbers in Fig. 4. The values of $\langle H\rangle$ are obtained by averaging H over y. The experimental data in Figs. 4 and 5 show that there is a range of values of the parameter Π_1 in which H is uniformly distributed along y, and $\langle H\rangle/h_* = \text{const} = 3$. For small and large values of Π_1, there were deviations from this dependence. For small Π_1, the influence of the lateral walls of the channel was manifested. For large Π_1, the continuity of the liquid jet rising on the wall was violated.

For adequate mathematical modeling of the problem considered, information on the internal structure of the flow is of great significance. Experimental data are partly given in [9]. These data demonstrate that a bore propagating over a counterflow generates a strong stratification in the liquid particle velocity. A thick boundary layer of the stagnated liquid is formed at the bottom, and large vortices are formed at the free surface. A wavy jet propagates in the flow region at the middle height. When the bore propagates over a quiescent liquid, the flow structure is simpler than that [9].

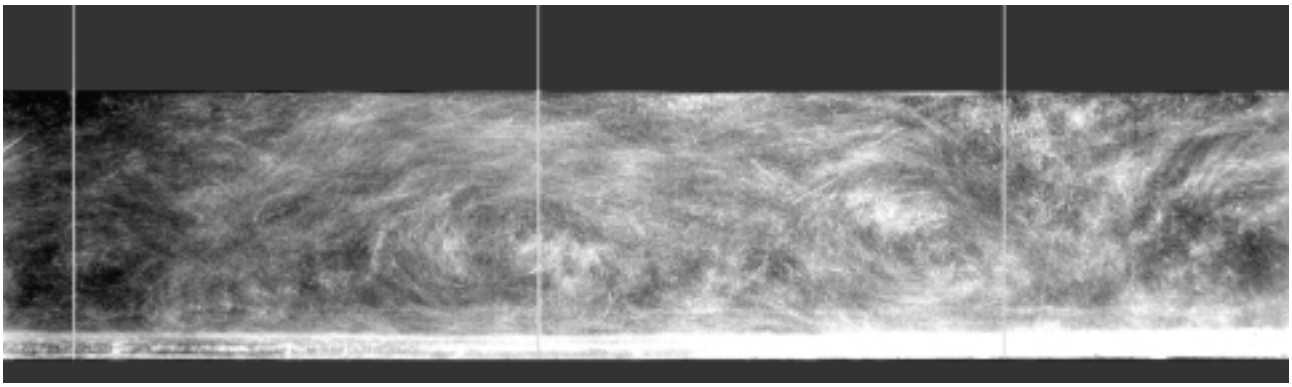

Fig. 6. Flow structure at a large distance from the bore front ($\Pi_1 = 0.235$).

The photographs given in [9] show only the head of a bore. In the problem considered, after blockade of the flow, the liquid continued to pass into the channel with flow rate Q, the free surface level behind the leading front of the bore increased continuously, and a decrement curve formed in the direction opposite to that in the unperturbed state. As a result, the internal structure of the flow remained complex at large distances from the leading front as well (Fig. 6). The vertical white lines on the photograph represent the scale grid on the internal surface of the lateral wall of the channel. The left line corresponds to a distance from the shield $x = 70$ cm. Here the depth of the unperturbed flow was 3.4 cm. The scale lines are spaced 10 cm apart. The exposure was 1 sec. At the beginning of filming, the leading front of the wave was at about $x = 160$ cm, and at the end, it was at about $x = 200$ cm. On this segment, the breaking of the leading front ceased. The free surface profile behind the bore was close to the that presented in Fig. 2 (curve 3).

From Fig. 6 one can see that ordered vortex structures are formed at large distances behind the leading front of the bore. Here, in contrast to the bore head, vortices are located at the middle height the flow region. This is due to the global circulation of the liquid between the bore head and the shield because the liquid passed continuously with constant flow rate Q through the leading front of the bore, and the rate of flow through the shield was equal to zero. The reverse flow from the shield to the front of the bore is concentrated in a thin layer at the free surface. The boundary layer at the bottom is thinner than that at the bore head.

In conclusion, it should be noted that the problem considered can be used to test and develop mathematical models capable of describing processes with distinct deterministic and random properties. In turbulence theory, much attention has been given to coherent (deterministic) structures, similar to those given in Fig. 6 (see, e.g., [10]). Recently, a number of mathematical models for describing the processes considered have also been proposed in wave theory. Such models must take into account the liquid particle velocities stratification. When shallow water theory is used in the standard Lagrangian approximations [11], the vertical velocity profile is approximated by polynomials, and, therefore, many terms of the series are required to describe vortex and jet flows. Calculations using the Euler or Navier–Stokes equations are simpler; the more so since there are appropriate algorithms (see, e.g, [12]). However, analytical studies of the general properties of flows using such numerical experiments are difficult. They provide less information than physical experiments because they can be used in a limited range of problem parameters.

New trends in shallow water wave theory (see, e.g., [13–15]) make analytical studies possible. This is achieved by using nonstandard methods of taking into account the nonhydrostatic pressure distribution along the vertical [13] or the vorticity [14, 15]. The experimental data presented here allow one to test these models not only for the shape, propagation speed, and height of bores but also for the internal structure of flows.

This work was supported by the Russian Foundation for Fundamental Research (Grant No. 98-01-00750) and the Program of Integration Fundamental Research of the Siberian Division of the Russian Academy of Sciences (Grant No. 2000-1).

REFERENCES

1. J. J. Stoker, *Water Waves. Mathematical Theory and Applications*, Interscience Publishers, New York (1957).
2. J. Tsuji, T. Januma, and I. Murata, "Tsunami ascending in rivers as an undular bore," *Natur. Hazards*, **4**, Nos. 2/3, 257 (1991).
3. P. G. Kiselev, *Manual on Hydraulic Calculations* [in Russian], Gosénergoizdat, Moscow–Leningrad (1957).
4. Ven Te Show, *Open-Channel Hydraulics*, McGraw-Hill, New York (1959).
5. V. I. Bukreev, "On the correlation between theoretical and experimental solitary waves," *Prikl. Mekh. Tekh., Fiz.*, **40**, No. 3, 44–52 (1999).
6. M. S. Longuet-Higgins and J. D. Fenton, "On the mass, momentum, energy, and circulation of a solitary wave. 2," *Proc. Roy. Soc., London*, **A340**, 471–493 (1974).
7. C. J. Amick and J. F. Toland, "On solitary water-waves of finite amplitude," *Arch. Rat. Mech. Anal.*, **76**, No. 1, 9–95 (1981).
8. V. I. Bukreev and A. V. Gusev, "Waves in a channel ahead of a vertical plate," *Izv. Ross. Akad. Nauk, Mekh. Zhidk. Gaza*, No. 1, 82–90 (1999).
9. V. I. Bukreev, "Undular bore on a counterflow," *Dokl. Ross. Akad. Nauk*, **373**, No. 6, 759–761 (2000).
10. H. Aref, "Integrable, chaotic, and turbulent vortex motion in two-dimensional flows," *Annu. Rev. Fluid Mech.*, **15**, 345–389 (1983).
11. L. V. Ovsyannikov, N. I. Makarenkov V. I. Nalimov, et al, *Nonlinear Problems of the Theory of Surface and Internal Waves* [in Russian], Nauka, Novosibirsk (1985).
12. C. M. Lemos, "Higher-order schemes for free surface flows with arbitrary configurations," *Int. J. Numer. Methods Fluids*, **23**, No. 6, 545–566 (1996).
13. V. Yu. Liapidevskii, "Shallow-water equations with dispersion. Hyperbolic model," *Prikl. Mekh. Tekh. Fiz.*, **39**, No. 2, 40–46 (1998).
14. T. B. Benjamin, "The solitary wave on a stream with an arbitrary distribution of vorticity," *J. Fluid Mech.*, **12**, Part 1, 97–116 (1962).
15. V. M. Teshukov, "Nonstationary interaction of uniformly swirled flows," *Prikl. Mekh. Tekh. Fiz.*, **39**, No. 5, 55–66 (1998).